Indian Journal of Chemical Technology
Vol. 33, March 2026, pp. 235-245
DOI: 10.56042/ijct.v33i2.21875

Sustainable management of agro industrial waste as potential adsorbent for wastewater treatment: Kinetic, thermodynamic and equilibrium study

Pradeep Kumar Ramteke[1], Ajit P. Rathod[1]*, S.M. Kodape[1] & A. W. Deshmukh[2]

[1]Department of Chemical Engineering, Visvesvaraya National Institute of Technology, Nagpur-440010 (MS), India

[2]Department of Chemical Engineering, SGGS Institute of Engineering & Technology, Nanded-431606 (MS), India

*E-mail: aprathod@che.vnit.ac.in

Received 22 July 2025; accepted 13 February 2026

In the current work, the malachite green (MG) dye was removed from synthetic wastewater by employing a sustainable adsorbent, Cajanuscajan (Tur dal husk) as an adsorbent. The activated carbon based on Tur dal husk has been prepared and characterized using Brunauer-Emmett-Teller analysis, scanning electron microscopy, and Fourier transform infrared spectroscopy techniques. The impacts of multiple causes, specifically pH, adsorbent quantity, contact duration, and the concentration of dye, have been investigated on the elimination of MG dye. The equilibrium isotherms underwent analysis through the Freundlich and Langmuir models. The highest ability to absorb is obtained as 24.81 mg/g, 30.95 mg/g, and 36.49 mg/g at 303K, 313K, and 323K, respectively. The separation factor value confirmed that the adsorption is beneficial at the adsorption conditions. The kinetics exhibited behavior consistent with pseudo-second-order kinetics. The thermal variables, involving entropy, Gibbs free energy, and enthalpy, revealed that adsorption is a process that occurs naturally and absorbs heat during the process.

Keywords: Adsorbent, Cajanuscajan, Malachite Green, Tur Dal Husk (TDH), Wastewater treatment

Introduction

More than 10,000 commercial dyes are available in the market and are extensively used in industries such as paper and pulp, leather processing, cosmetic formulation, dyeing processes, plastics, and the food industry[1,2]. The consumption of dyes in these industries is increasing every year, and even at very low concentrations, textile dyes exhibit substantial toxicity, being both carcinogenic and mutagenic[3]. According to literature reports, over 7×10^5 tonnes of wastewater are generated annually by textile industries[4]. The disposal of such wastewater poses a serious environmental challenge because it contains organic pollutants that significantly increase chemical oxygen demand (COD) and biochemical oxygen demand (BOD), thereby affecting aquatic ecosystems and water quality[5]. The dye examined in the present study is malachite green (MG), a water-soluble cationic dye belonging to the triphenylmethane group. MG is widely used as an antifungal and antiprotozoal agent in aquaculture and for coloring materials such as wool, cotton, and leather[6]. However, MG is highly toxic to mammalian cells, acts as a tumor-promoting substance, and exhibits mutagenic and carcinogenic effects once it enters the food chain[7,8]. Furthermore, carcinogenic by-products are formed during its degradation, leading to its ban in several countries, including Japan and the United States[9]. These concerns necessitate the development of effective and sustainable methods for MG removal from wastewater.

Various techniques have been explored for dye removal from wastewater, including coagulation, filtration, biological treatment, flocculation, precipitation, electro-floatation, ion exchange, photodegradation, photocatalytic degradation, advanced oxidation processes, and adsorption[10]. However, many of these methods suffer from limitations such as high operational cost, excessive energy demand, and large sludge generation. Among these techniques, adsorption is widely recognized as one of the most efficient, simple, and economical methods for wastewater treatment[11]. Additionally, adsorption enables the recovery of valuable or toxic substances from wastewater, making it particularly attractive for industrial applications[12].

Activated carbon is commonly used as an adsorbent for dye removal at the commercial level; however, its high production cost limits large-scale application. Consequently, recent research has

focused on the development of low-cost adsorbents derived from natural and agricultural by-products, which are abundantly available and economically viable[13]. Several agro-waste materials such as biomass fly ash[14], rice straw-derived char[15], neem leaf powder[16], banana pith[17], banana and orange peels[18], soyabeen hull[19], chitosan/oil and palm ash[20], sunflower seed hull[21], have been successfully investigated for dye removal from wastewater. A comprehensive list of such low-cost adsorbents has been compiled by Crini[22]. While chemical activation methods are often reported to enhance adsorption capacity, they are associated with higher chemical consumption, secondary wastewater generation, and increased processing cost[23]. Tur dal husk (TDH) is an agro-industrial waste generated in large quantities from dal mills and is primarily used as cattle feed. During processing, it is often treated with alkali, lime water, and other chemicals, which may render it unsuitable for animal consumption. Despite its carbon-rich nature and abundant availability, TDH remains largely underutilized for environmental remediation applications. The utilization of TDH for activated carbon preparation using a simple thermal activation route can therefore offer a sustainable and environmentally benign alternative to chemically activated carbons [24]. In this context, the present study explores the use of TDH as a low-cost adsorbent for the removal of malachite green dye from synthetic wastewater.

The objectives of this study are to prepare activated carbon from TDH using a simple thermal activation route and to systematically evaluate its adsorption performance toward MG dye. The effects of key operational parameters such as solution pH, adsorbent dose, contact time, dye concentration, and temperature are investigated. The adsorption behaviour is analyzed using kinetic, equilibrium isotherm, and thermodynamic models, and the adsorption mechanism is interpreted using surface characterization techniques. This work aims to contribute toward the development of environmentally benign and practically viable adsorbents for wastewater treatment applications, particularly for dye-contaminated effluents [5].

Although agro-waste-derived activated carbons have been widely investigated for malachite green adsorption, the present study offers distinct contributions in terms of precursor selection, preparation route, and application-oriented evaluation. TDH, an abundantly available agro-industrial residue, has been scarcely explored as a precursor for the preparation of activated carbon for dye removal applications. In contrast to many reported studies that employ chemical activation to enhance adsorption capacity, the activated carbon in this work was prepared using a simple thermal activation route without chemical activating agents, thereby reducing chemical consumption, secondary wastewater generation, and processing complexity. Despite the absence of chemical activation, the TDH-based activated carbon exhibits satisfactory adsorption performance, along with favourable kinetic and equilibrium behaviour. The present study, therefore, demonstrates that thermally activated TDH can serve as a low-cost and environmentally benign adsorbent, contributing to the development of sustainable materials for wastewater treatment.

Experimental Section

Adsorbate preparation

The malachite green (MG) dye, with the chemical formula $C_{52}H_{54}N_4O_{12}$, a molecular weight of 927 g/mol, also known as basic green 4, designated as C.I. No. 42000, and having a maximum absorption wavelength (ʎmax) of 616.9 nm, was provided by LOBA Chemie Pvt. Ltd. A 100 mg/L The dyes stock solution was created using deionized water, and solutions of desired concentrations were formulated using this stock solution.

Adsorbent preparation

Tur dal husk (TDH) was obtained from a pulse processing facility situated in Nagpur. Initially, it underwent a set of preparation steps. It was first cleaned with double-distilled water, then tap water to eliminate any dust particles. Afterward, it was sun-dried and further dehydrated in a heating oven set at approximately 110°C for a duration of 8 h to reduce its moisture content. The material was subsequently crushed and sifted to obtain particles within the size range of 50 to 100 µm. Following this, carbonization was carried out using a muffled furnace at around 450°C for a span of 4 h. The subsequent treatment involved using concentrated hydrochloric acid (HCl) to eliminate ash content from the carbon, followed by repeated rinsing withdouble-distilled water, achieving a pH of 7. The material was then subjected to another drying phase in a heating oven at 110°C for 8 h to extract any remaining moisture content. Ultimately,

activation was achieved bysubjecting the material to a temperature of 450°C for duration of 4 h in a muffle furnace. The complete sequence of steps is depicted in Fig. 1.

Physical and chemical characterization

A scanning electron microscope (SEM) was employed to capture the morphological composition of TDH before and subsequent to the adsorption of MG dye. Fourier transform infrared spectroscopy (FTIR) spectrum was conducted to determine the groupings of functions that are present, encompassing the range of the scanning between 400-4000 cm^{-1}. The area of the surface adsorbent was assessed through the utilization of the Brunauer-Emmett-Teller (BET) Smart sorb 92/93 equipment.

Adsorption study

Batch-mode adsorption experiments were executed utilizing 250 mL conical flasks, each having dye solution in a 100 mL volume. The experiments were conducted at varied temperatures (303K, 313K, and 323K), various concentrations of the dye (30, 60, and 80 mg/L), diverse pH levels ranging from 3 to 9, and varying adsorbent doses spanning 1 to 6 g/L of the solution of dye. After agitation for the designated duration, the mixture was filtered, and the MG supernatant's dye concentration was quantified employing a UV-spectrophotometer (Jasco V530) by measuring the 618 nm absorbance, which showed the highest level of dye absorption efficiency. A calibration curve was established through the utilization of known MG dye concentrations. The dye separation percentage (% R) and the quantity of dye adsorbed onto the surface of TDH (q_e in mL/g) were established by employing Eqs (1) and (2), respectively.

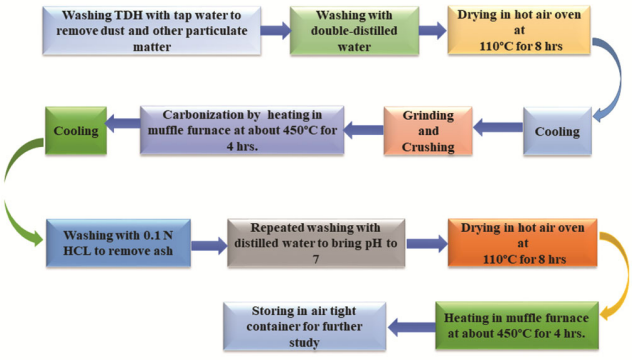

Fig. 1 — Schematic representation of procedure for the preparation of activated carbon from TDH

$$\% R = \frac{(C_o - C_e)}{C_o} \times 100 \quad \ldots(1)$$

$$q_e = \frac{(C_o - C_e) \times V}{M} \quad \ldots(2)$$

where, C_o is initial dye concentration of the mixture (mg/L), while C_e denotes the dye concentration at equilibrium (mg/L). V is the amount of the solution in L, and M represents the quantity of the material used for adsorption in g, respectively.

Adsorption isotherms

The adsorption isotherm provides information about how molecules are distributed between the adsorbed states in both solid and liquid states. The equations for Langmuir and the Freundlich[25] isotherms are shown in Eqs (3) and (4), respectively.

$$\frac{C_e}{q_e} = \frac{1}{q_m \times K_L} + \frac{C_e}{q_e} \quad \ldots(3)$$

$$\ln q_e = \ln k_f + \frac{1}{n} + \ln C_e \quad \ldots(4)$$

where, C_e refers to the appropriate amount of dye within the mixture (ml/L), q_e signifies the adsorbent dye concentration (mL/g), q_m denotes the highest adsorption capability achievable by the adsorbent (mg/g), K_L stands for the Langmuir value (L/mg), while k_f and n are the Freundlich constants. The Langmuir constant, denoted as $k_{L,}$ is utilized to forecast the desirability of the adsorption procedure by employing the factor of separation $R_{L,}$ which is determined by the Eq. (5) [26].

$$R_L = \frac{1}{1 + k_L \times C_o} \quad \ldots(5)$$

The adsorption isotherm is deemed unfavorable when the separation factor R_L is higher than 1, linear when R_L equals 1, positive when R_L falls within 0 and 1, and irreversible whenever R_L is equal to 0.

Adsorption kinetics

The study examined the adsorption kinetics of MG dye using Ho's pseudo-second-order and Lagergren's pseudo-first-order kinetic models, applying the respective Eqs (6) and (7).

$$\ln(q_e - q_t) = \ln q_e - k_1 \times t \quad \ldots(6)$$

$$\frac{t}{q_t} = \frac{1}{k_2 \times q_e^2} + \frac{t}{q_e} \quad \ldots(7)$$

In this context, q_t (mg/g) represents the quantity of absorbed dye over time t (min), k_1 (min^{-1}) signifies the

rate determinant for the pseudo-first-order reaction, and k_2 (g/mg.min) signifies the pseudo-second-order reaction's rate coefficient. The interparticle diffusion was determined by using Eq. (8).

$$q_t = k_i \times t^{0.5} + C \quad \ldots(8)$$

In this context, k_i (mg/g.min$^{0.5}$) stands for the rate determinant of interparticle diffusion, and C (mg/g) denotes the deviation.

Thermodynamic adsorption

The thermodynamic characteristics, consisting of alteration in Gibbs free energy, denoted as ΔG in units of J/mol, entropy alteration represented as ΔS in J/mol·K, and the modification in enthalpy denoted as ΔH in J/mol, were assessed utilizing Eqs (9) and (10) [12].

$$\Delta G = \Delta H - T \times \Delta S \quad \ldots(9)$$

$$\ln k_D = \frac{\Delta S}{R} - \frac{\Delta H}{R \times T} \quad \ldots(10)$$

In this equation, k_D is defined as the ratio of q_e to C_e, where C_e represents the equilibrium condition (mg/L) of A solution containing MG dye, q_e (mg/g) represents the quantity of dye on the adsorbent, and the standard gas constants are denoted by R, which is 8.314 J/(mol·K).

Results and Discussion

Characterisation of the adsorbent

SEM analysis

SEM micrographs shown in Fig. 2 shows the adsorbents' condition both before and following the adsorption of MG dye. Before adsorption (Fig. 2a), pores and cavities were observed, while after adsorption (Fig. 2b) the pores are not visible indicating the adherence of MG dye to the adsorbents' pores.

FTIR analysis

The adsorption of the dye onto TDH-based activated carbon adsorbent occurs through multiple interacting mechanisms rather than a single process. FTIR analysis confirms the presence of surface functional groups such as –OH, C=O, and C=C, which actively participate in dye binding through hydrogen bonding and surface complexation. The FTIR spectrum of the adsorbent was recorded the adsorption on before and after the MG dye and are presented in Fig. 3. The FTIR spectrum of the adsorbent, as displayed in Fig. 3a, reveals the existence of several functional groups. The stretching of C-H bonds is indicated by the peak at 3050 cm^{-1}, at 2860 cm^{-1} to the elongation of (CO)-H bonds, at 2116 cm^{-1} to the elongation of C=C bonds, and at 1887 cm^{-1} to the stretching of C=O bonds. When activated carbon was treated with MG dye, as seen in Fig. 3b, a shift in the bands was observed: 3053 cm^{-1} is indicative of stretching of C-H bonds, 2881 cm^{-1} corresponds to the elongation of (CO)-H bonds, 2114 cm^{-1} corresponds to the stretching of C=C bonds, and 1842 cm^{-1} coincides with the stretching of C=O bonds[27–30].

BET analysis

In the present study, the surface area of the adsorbent was calculated to be 385.31 m²/g. This large

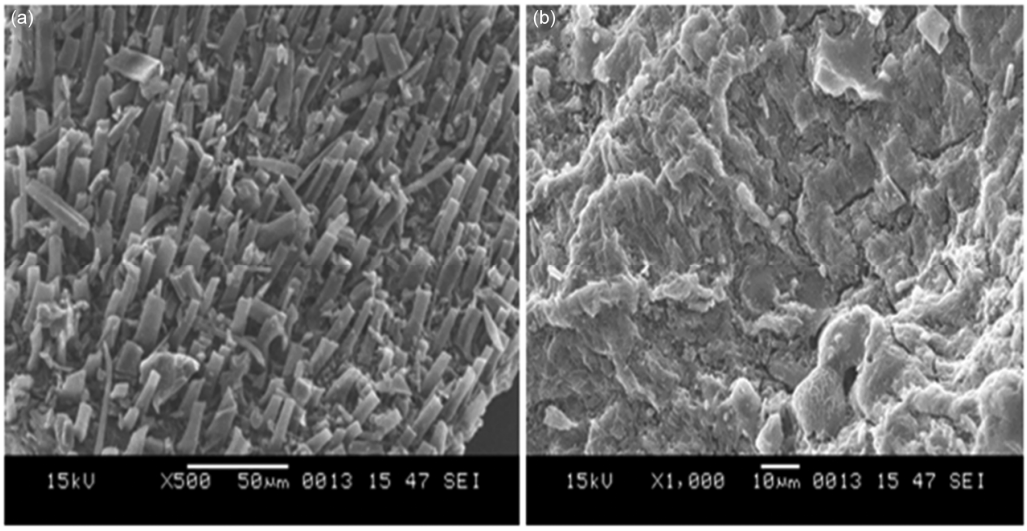

Fig. 2 — SEM micrographs of TDH based activated carbon (a) before and (b) after the dye adsorption

size of the surface reveals that the TDH-based activated carbon possesses significant adsorbent capacity.

Adsorption of dye as a function of solution pH

The pH of the solution influences the aqueous chemistry and the adsorbent's surface-bounding elements. The effect of pH within a pH range 3-9 on the adsorption capacity of the adsorbent was studied at a fixed dye concentration dye of 80 mg/L, shaking time 120 min, temperature 303K, and the adsorbent dose 5 g/L. The impacts of pH are represented in Fig. 4. The results indicated that the removal percentage of MG dye was a minimum value (46.83%) when the pH of the solution was 3, and it reached a maximum value (86-87%) when the pH was between 8-10. Beyond pH 8, the removal percentage of the dye remains unchanged. Therefore, pH 8 was fixed for the adsorption study.

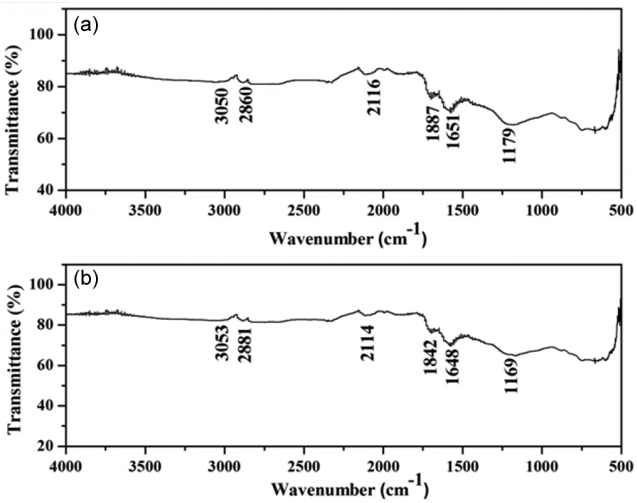

Fig. 3 — FTIR spectra of the adsorbent (a) before and (b) after adsorption

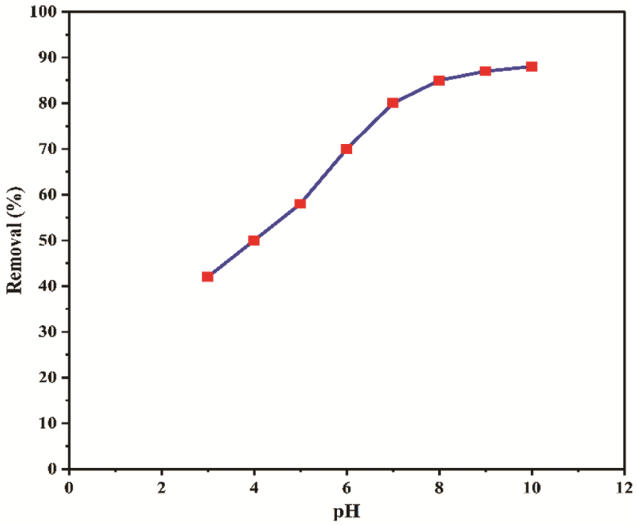

Fig. 4 — Adsorption efficiency of adsorbent as a function of solution pH

At low pH, the removal percentage of MG dye was low. This can be explained by the increase in concentration of H^+ ions at acidic pH, which competes with positively charged dye ions and consequently reduces the quantity of dye removal. At pH 8 or above, there is a rise in the quantity of surface groups carrying negative charges on the adsorbent. This augmentation amplifies the adsorption of cations from positively charged dyes via the attractive electrostatic force.

Impact of the contact duration and dye concentration on dye adsorption

The duration of approach between the amount of dye, the adsorbent, and the adsorbate present in the mixture influences the removal percentage of the solution's MG dye. To investigate this, a study was conducted at pH 8, utilizing a 0.5 g dose of the adsorbent and a temperature of 303K. Fig. 5 illustrates the removal percentage of dye for solution concentrations of 30, 60, and 80 mg/L at various contact times.

The percentage of dye removal reached the maximum at 150 min and it was 97.83%, 96.84%, and 93.78% for 30, 60, and 80 mg/L, respectively. Hence, 150 min was fixed for the adsorption study. The Figure illustrates that the removal efficiency is swift at the beginning and gradually diminishes in the later stages until it reaches a state of saturation. This is because of the fact that at the initial stages, huge numbers of sites of activity are present for the dye adsorption. However, as time progressed, the quantity

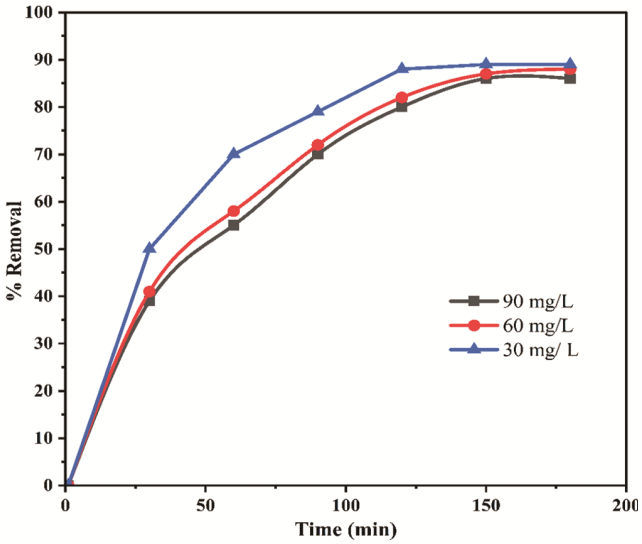

Fig. 5 — Impact of contact time and dye concentration on dye adsorption

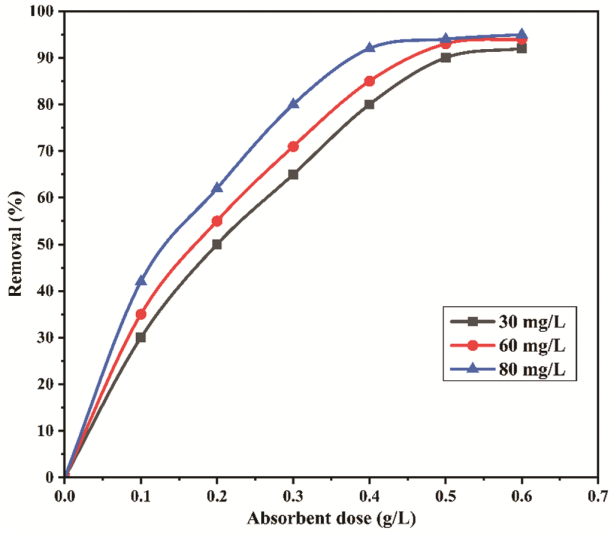

Fig. 6 — Effect of adsorbent dose on the dye removal efficiency

of available sites reduced, and it became difficult to occupy the remaining sites experienced repulsion due to the interaction among the molecules of the substance present in both the solid and bulk phases. The reduction in dye removal percentage was observed to decline as the dye concentration increased, a phenomenon that can be illustrated by the point at which the surface's adsorption sites become fully occupied.

Effect of adsorbent dose on dye adsorption

The effect of adsorbent was observed at a pH of 8, connecting time of 150 min, and temperature of 303K onto the dye solute with a particular concentration of 60 mg/L by changing the adsorbent quantity from 1-6 g/L, and the result is shown in Fig. 6. The results indicated that when the quantity of adsorbent increases, the viability of dye removal also increases. The percentage of removal dye experienced a substantial increase from 38.93% to 96.84%, as the quantity of adsorbent material used was raised from 0.1 g/L to 0.5 g/L. Although as the adsorbent dose continued to rise, the percentage removal remained relatively constant. Hence, 0.5 g/L of adsorbent dose was fixed for further adsorption experiments. The adsorption was increased by the increase in adsorbent dosage, and as a result, the dye removal percentage increased.

Adsorption isotherm investigation

The interaction between the adsorbent and MG dye was investigated by examining adsorption isotherms, specifically Langmuir and Freundlich isotherms, at various temperatures (303K, 313K, and 323K).

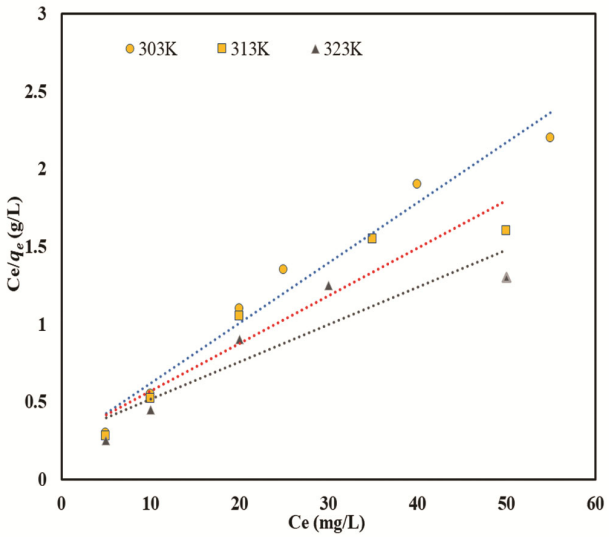

Fig. 7 — Langmuir isotherm for MG dye adsorption

Table1 — The removals isotherm parameter of different temperatures for MG dye

Isotherms	Parameters	Temperature (K)		
		303	313	323
Langmuir	Q_{max} (mg/g)	24.81	30.95	36.49
	k_L (L/mg)	0.2238	0.1435	0.1175
	R_L	0.0558	0.0870	0.1063
	R^2	0.92	0.91	0.93
Freundlich	k_F (mg/g(L/mg)$^{1/n}$)	10.92	9.76	9.14
	N	5.38	3.84	3.17
	R^2	0.97	0.93	0.92

Langmuir isotherm

The graphs of C_e/q *vs* C_e were plotted at 303K, 313K, and 323K, which exhibited the linear trends as observed in Fig. 7. The values of the correlation coefficient (R^2) acquired for the tested plots were as follows: 0.97 at 303K, 0.93 at 313K, and 0.92 at 323K. Such a large correlation coefficient value revealed the good fit of Langmuir's isotherm model which states the monolayer formation and uniform dispersion of dye at the adsorbents surface[27]. The value of Q_{max} and k_L was obtained from slope and intercept of the graph and is reported in Table 1. The separation factor's numerical value, R_L, was evaluated and obtained to be 0.055, 0.087, and 0.10 at temperatures of 303K, 313K, and 323K, respectively, and it lies between 0 to 1. According to these findings, the adsorption of MG dye was advantageous inside the specified adsorption situations.

As shown in Table 2, several thermally activated or raw natural adsorbents exhibit adsorption capacities of 15–32 mg g^{-1}, which are comparable to or lower than that of the present TDH-based activated carbon

Table 2 — List of different thermally activated and raw natural adsorbents reported in the literature

Adsorbent / Biomass	Activation / Modification	Adsorbate	Isotherm	Qmax (mg g^{-1})	Ref.
Walnut-shell AC loaded magnetic nanocomposites	Pyrolysis, nanocomposite	Methyl orange, Methylene blue	Langmuir	345.7	31
ZnO/activated carbon khat nanocomposite	Composite with ZnO	Methylene blue	Freundlich (MB)	-	32
Pineapple peel/sawdust AC *(agro-waste)*	Chemical & thermal	Methylene blue	Langmuir/Freundlich	-	33
Agro-waste AC *(MB and MG)*	Agro-waste AC	Methylene blue	Freundlich	-	34
Vigna mungo & Paspalum scrobiculatum AC	Pyrolysis & activation	Methylene blue	Isotherm studies	-	35
Geranium plant waste biosorbent	Untreated biosorbent	Methylene blue	Langmuir / Freundlich	-	36
Paulownia wood $ZnCl_2$-activated AC	$ZnCl_2$ chemical	Methylene blue	Langmuir	322.6–384.6	37
Pepper stem AC	Microwave-assisted impregnation	Methylene blue	Langmuir	178.4	38
Mesquite sawdust AC	Chemical activation	Methylene blue	Langmuir	~1.76 (minor)	39
BAC from almond shell / walnut shell ACs (literature)	H_3PO_4 / KOH activation	Methylene blue	Langmuir	~100+ typical	40
Rice straw & palm oil midrib AC (composite)	Chemical	Naphtol – similar; MB analog	Langmuir	55.9 / 69.4	41
Activated carbon	Millet cob husk	Basic dye	Langmuir, Freundlich	18.2	42
Palm tree male flower	Chemical	Methylene blue	Langmuir isotherm	143.6–157.31	43
Neem leaf powder	Neem leaves	Malachite green	Freundlich	6–12	16
Microwave-assisted activated carbon	Okra stalk waste	Malachite green	Langmuir	119.05	44
H_3PO_4-impregnated activated carbon	*Rumex abyssinicus* stem	Malachite green	Langmuir, Freundlich	98.43	45

(Q_{max} = 24.81–36.49 mg. g^{-1}). Although higher capacities reported in the literature are often achieved through chemical activation, the present thermally activated TDH-based adsorbent demonstrates competitive performance with simpler processing, lower cost, and improved sustainability.

Freundlich isotherm

The graphs of ln(q_e) *vs* ln(C_e)were plotted at 303K, 313K and 323K which shows linear trends as presented in Fig. 8. The correlation coefficient (R^2) values were found to be 0.92, 0.91, and 0.93 at 303K, 313K, and 323K, respectively. Such elevated correlation coefficient values demonstrate the good fit of the Freundlich model [46]. The Freundlich constant n and k_f were calculated based on the slope and intercept of the graph, and their values are reported in Table 1. The values of n, greater than 1, elucidate that the dye adsorption exhibits both favourability and heterogeneity.

Kinetic adsorption

The adsorption constant rate (k_1) of MG dye using TDH was found using Lagergren's first-order kinetics. The graph of (-ln(q_e-q_t)) vs t was plotted at 303K as shown in Fig. 9. The graph shows linear trends. The coefficient of correlation (R^2) was

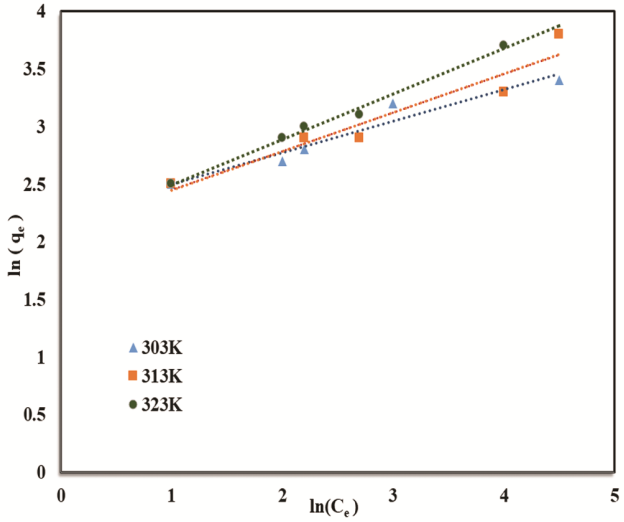

Fig. 8 — Freundlich isotherm for MG dye adsorption

determined to be 0.87, 0.82, and 0.94 for dye concentrations 30 mg/L, 60 mg/L, and 80 mg/L. The value of k_1 was assessed from the graph's slope and intercept and is documented in Table 3.

To study Ho's model for the kinetics at second order, a graph plotting t/q_t vs. t was created as presented in Fig. 10 and the correlation coefficient (R^2) was estimated to be 0.99, 0.99, 0.99 for 30, 60, and 80 mg/L dye solution, respectively. The coefficients of

Table 3 — Comparing the calculated qe values for the initial concentration of MG dye (Co)and the first- and second-order pseudosystem reactions' rate constants

C_o (mg/L)	Pseudo-first-order kinetics			Pseudo-second-order kinetics			Interparticle diffusion		
	q_1 (mg/g)	k_1 (min^{-1})	R^2	q_2 (mg/g)	k_2 (g.mg/min)	R^2	k_i ($mg/g.min^{0.5}$)	C (mg/g)	R^2
30	2.71	0.0387	0.82	7.24	0.003624	0.99	0.3515	1.52	0.93
60	3.93	0.0436	0.87	16.23	0.000917	0.99	0.8528	0.80	0.98
80	4.50	0.0283	0.94	22.32	0.000557	0.99	1.1855	0.073	0.97

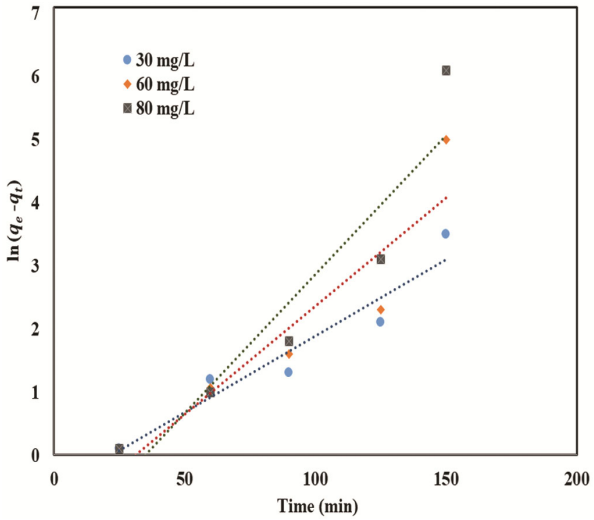

Fig. 9 — Lagrergren's pseudo first order kinetics for adsorption of MG dye

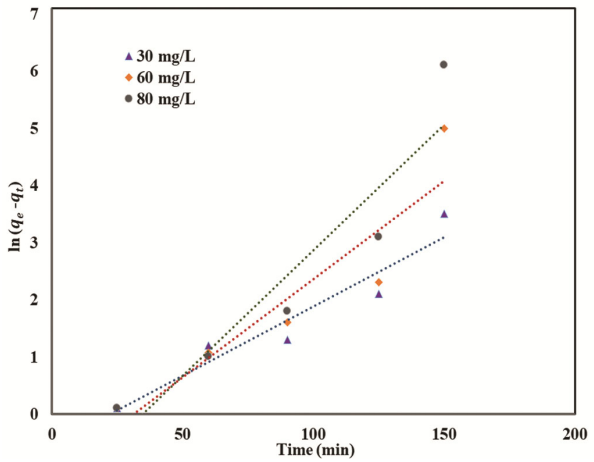

Fig. 10 — Ho's pseudo second order kinetic model for adsorption of MG dye

correlation for Ho's model were more than those for Lagregen's model, demonstrating that the procedure of adsorption conforms to the model for kinetics of pseudo-second order. The findings demonstrating that chemisorption is likely the step that establishes the general rate in the adsorption of MG dye[23].

Interparticle diffusion study

The graph of q_e vs. $t^{0.5}$ was plotted for 30, 60, and 80 mg/L dye solution at 303K as represented in

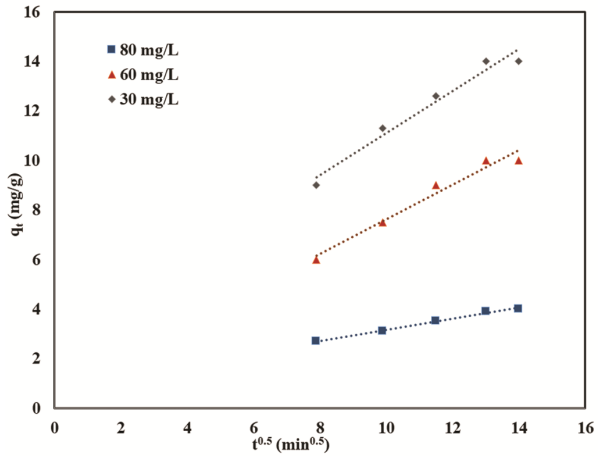

Fig. 11 — Model of diffusion applied to the adsorption of MG dye

Fig. 11. If the graph is a linear trajectory that goes through the point of origin, it suggests that interparticle diffusion is important in the adsorption in a process. However, if this line doesn't intersect the origin, it suggests that other processes, in addition to interparticle diffusion, may be influencing the rate of adsorption.

The correlation coefficient (R^2) values were discovered to be 0.93, 0.98, and 0.97 for 30 mg/L, 60 mg/L and 80 mg/L dye solution. The values of C and k_i were established based on the gradient and intercept of the graph and are provided in Table 2. The graph is a line that is straight and does not cross over the source which demonstrates that interparticle diffusion represents more than just the step that limits the rate. The values of C for all dye solutions were obtained to be positive which indicating that the experimental values must be fitted with a diffusion model external.

Adsorption thermodynamics

The thermodynamic characteristics, such as changes in entropy, enthalpy, and Gibbs free energy (ΔS, ΔH, and ΔG), were determined using Eqs (8) and (9). Fig. 12 shows the graph of ln (K_D) against 1/T, from which the values of ΔH and ΔS were obtained by analyzing the y-intercept and slope. The values of

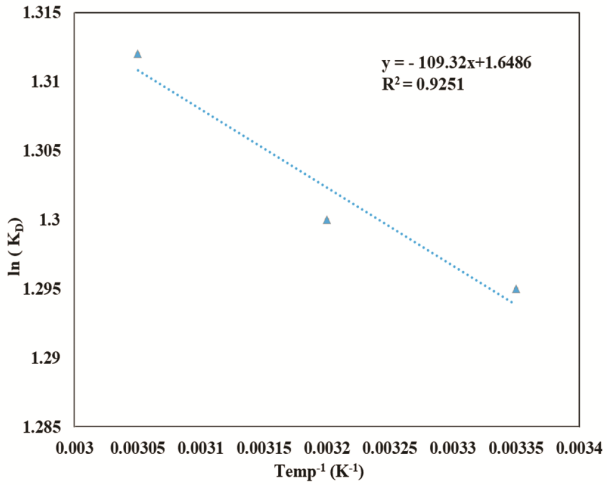

Fig. 12 — Graph of ln (K_D) vs 1/T for MG dye adsorption

ΔG were evaluated to be -3.244, -3.381, and -3.518 kJ/mol at 303K, 313K, and 313K, respectively. The values of ΔH and ΔS were discovered to be 908.88 J/mol K and 13.70 J/mol, respectively. The ΔH value is positive suggesting that the adsorption procedure of MG dye is characterized as endothermic [47]. The value of ΔS was positive which elucidates that the process of adsorption of MG dye occurs due to energy re-distribution between dye and TDH.

Adsorbent regeneration and reuse

For practical wastewater treatment applications, the regeneration and reuse of adsorbents are critical for reducing operating costs and minimizing secondary waste generation. Biomass-derived activated carbons similar to the present TDH-based material have been reported to be regenerable using simple methods such as thermal treatment or solvent washing, with acceptable retention of adsorption capacity over multiple cycles [15]. Given the thermal stability of carbonaceous adsorbents, the TDH-based activated carbon is expected to tolerate regeneration through moderate heating or solvent-assisted desorption. Although regeneration experiments were not included in the present study, the literature indicates that 3–5 adsorption–desorption cycles are commonly achievable for agro-waste-derived activated carbons before a noticeable decline in performance occurs [22]. This suggests promising potential for reuse, which will be explored in future work.

Cost considerations

From a techno-economic perspective, the present adsorbent offers notable advantages. The raw material TDH is an abundantly available agro-industrial waste, and the preparation process involves only thermal activation, thereby avoiding the use of chemical activating agents. Although chemical activation methods (e.g., KOH or H_3PO_4) are known to significantly enhance adsorption capacity, they are associated with higher material costs, extensive washing steps, secondary wastewater generation, and environmental concerns [12]. In contrast, the simpler thermal route adopted in this study reduces chemical consumption and processing complexity, making the TDH-based activated carbon economically attractive for large-scale or decentralized wastewater treatment applications, even with moderate adsorption capacity.

Applicability to real wastewater matrices

While the present study was conducted using synthetic malachite green solutions, real industrial wastewater typically contains competing ions, dissolved salts, natural organic matter, and multiple dyes, all of which can influence adsorption performance. Previous studies have reported that these matrix components may reduce adsorption efficiency due to site competition and pore blockage, particularly for cationic dyes [5]. Nevertheless, carbon-based adsorbents have demonstrated reasonable robustness in complex matrices, especially when electrostatic and π–π interactions jointly contribute to adsorption. Therefore, although a reduction in adsorption capacity may be expected in real wastewater, the TDH-based activated carbon is anticipated to remain effective. Future studies will focus on evaluating adsorption behavior in actual textile or dye-industry effluents to further assess real-world applicability. Overall, considering its regenerability, low-cost preparation, absence of chemical activation, and expected robustness in complex wastewater systems, the TDH-based activated carbon shows strong potential as a sustainable and practically relevant adsorbent for dye-contaminated wastewater treatment.

Conclusion

TDH was effectively utilized as form of MG dye hazardous waste removal adsorbent for synthetic wastewater. The characterization results elucidated that the TDH adsorbent possessed significant adsorption sites to perform of MG dye adsorption. The dye's adsorption increased with the build in pH, temperature and adsorbent dose. The data in equilibrium was examined utilizing the Langmuir and Freundlich models of isotherms. The highest possible

monolayer adsorption capability was obtained as 24.81 mg/g, 30.95 mg/g, and 36.49 mg/g at 303K, 313K and 323K, respectively. The value of separation factor was estimated and it lies in between 0 to 1 which stated that adsorption of dye was favourable under given adsorption study. The data followed Ho's kinetic model which demonstrated pseudo second order kinetics. The study of interparticle model of diffusion elucidated that interparticle not just diffusion was a rate limiting process. The thermodynamic parameter values (ΔG, ΔH, ΔS) showed that the adsorption procedure is both spontaneously and absorbs heat (endothermic). Thus, Tur Dal Husk carbon-based activated can be effectively employed as a sorbent for removing malachite green dye.

Conflict of interest

The authors declare that they have no conflict of interest.

Acknowledgments

We are thankful to the chemical engineering departments from Visvesvaraya National Institute of Technology Nagpur for providing experimental facilities.

References

1 Pereira A G B, Rodrigues F H A, Paulino A T, Martins A F & Fajardo A R, Recent advances on composite hydrogels designed for the remediation of dye-contaminated water and wastewater: A review, *J Clean Prod*, 284 (2021) 124703.
2 Kabdaçh I, Tünay O & Orhon D, Wastewater control and management in a leather tanning district, *Water Sci Technol*, 40 (1999) 261.
3 Ahmed M B, Zhou J L, Ngo H H & Guo W, Adsorptive removal of antibiotics from water and wastewater: Progress and challeng`es, *Sci Total Environ*, 532 (2015) 112.
4 Gupta V K, Pathania D, Agarwal S & Sharma S, De-coloration of hazardous dye from water system using chemically modified Ficus carica adsorbent, *J Mol Liq*, 174 (2012) 86.
5 Vyavahare G D, Gurav R G, Jadhav P P, Patil R R, Aware C B & Jadhav J P, Response surface methodology optimization for sorption of malachite green dye on sugarcane bagasse biochar and evaluating the residual dye for phyto and cytogenotoxicity, *Chemosphere*, 194 (2018) 306.
6 Moturi B & Charya M S, Decolourisation of crystal violet and malachite green by fungi, *Sci World J*, 4 (2010) 28.
7 Culp S J & Beland F A, Malachite green: A Toxicological review, *J Am Coll Toxicol*, 15 (1996) 219.
8 Srivastava S, Sinha R & Roy D, Toxicological effects of malachite green, *Aquat Toxicol*, 66 (2004) 319.
9 Cha C J, Doerge D R & Cerniglia C E, Biotransformation of malachite green by the fungus cunninghamella elegans, *Appl Environ Microbiol*, 67 (2001) 4358.
10 Bhaskar M, Gnanamani A, Ganeshjeevan R J, Chandrasekar R, Sadulla S & Radhakrishnan G, Analyses of carcinogenic aromatic amines released from harmful azo colorants by Streptomyces SP. SS07, *J Chromatogr A*, 1018 (2003) 117.
11 Sharma G, Naushad M, Al-Muhtaseb A H, Kumar A, Khan M R, Kalia S, Shweta, Bala M & Sharma A, Fabrication and characterization of chitosan-crosslinked-poly(alginic acid) nanohydrogel for adsorptive removal of Cr(VI) metal ion from aqueous medium, *Int J Biol Macromol*, 95 (2017) 484.
12 Gupta V K & Suhas, Application of low-cost adsorbents for dye removal-A review, *J Environ Manag*, 90 (2009) 2313.
13 Nguyen T A H, Ngo H H, Guo W S, Zhang J, S Liang, Yue Q Y, Li Q & Nguyen T V,. Applicability of agricultural waste and by-products for adsorptive removal of heavy metals from wastewater, *Bioresour Technol*, 148 (2013) 574.
14 Pengthamkeerati P, Satapanajaru T & Singchan O, Sorption of reactive dye from aqueous solution on biomass fly ash, *J Hazard Mater*, 153 (2008) 1149.
15 Hameed B H & El-Khaiary M I, Kinetics and equilibrium studies of malachite green adsorption on rice straw-derived char, *J Hazard Mater*, 153 (2008) 701.
16 Bhattacharyya K G & Sarma A, Adsorption characteristics of the dye, Brilliant Green, on neem leaf powder, *Dye Pigment*, 57 (2003) 211.
17 Namasivayam C, Prabha D & Kumutha M, Removal of direct red and acid brilliant blue by adsorption on to banana pith, *Bioresour Technol*, 64 (1998) 77.
18 Annadurai G, Juang R & Lee D, Use of cellulose-based wastes for adsorption of dyes from aqueous solutions, *J Hazard Mater*, 92 (2002) 263.
19 Chandane V & Singh V K, Adsorption of safranin dye from aqueous solutions using a low-cost agro-waste material soybean hull, *Desalin Water Treat*, 57 (2016) 4122.
20 Ahmad A A, Hameed B H & Aziz N, Adsorption of direct dye on palm ash: Kinetic and equilibrium modeling, *J Hazard Mater*, 141 (2007) 70.
21 Hameed B H, Equilibrium and kinetic studies of methyl violet sorption by agricultural waste, *J Hazard Mater*, 154 (2008) 204.
22 Crini G, Non-conventional low-cost adsorbents for dye removal: A review, *Bioresour Technol*, 97 (2006) 1061.
23 Blanco S P D M, Scheufele F B, Módenes A N, Espinoza-Quiñones F R, Marin P, Kroumov A D & Borba C E, Kinetic, equilibrium and thermodynamic phenomenological modeling of reactive dye adsorption onto polymeric adsorbent, *Chem Eng J*, 307 (2017) 466.
24 Maneerung T, Liew J, Dai Y, Kawi S, Chong C & Wang C H, Activated carbon derived from carbon residue from biomass gasification and its application for dye adsorption: Kinetics, isotherms and thermodynamic studies, *Bioresour Technol*, 20 (2016) 350.
25 Langmuir I, the constitution and fundamental properties of solids and liquids, *J Am Chem Soc*, 38 (1916) 2221.
26 Du X, Cheng Y, Liu Z, Yin H, Wu T, Huo L & Shu C, CO_2 and CH_4 adsorption on different rank coals: A thermodynamics study of surface potential, Gibbs free energy change and entropy loss, *Fuel*, 283 (2021) 118886.
27 Asemani M & Rabbani A R, Detailed FTIR spectroscopy characterization of crude oil extracted asphaltenes: Curve resolve of overlapping bands, *J Pet Sci Eng*, 185 (2020) 106618.

28 Sato H, Dybal J, Murakami R, Noda I & Ozaki Y, Infrared and Raman spectroscopy and quantum chemistry calculation studies of C-H-O hydrogen bondings and thermal behavior of biodegradable polyhydroxyalkanoate, *J Mol Struct*, 744 (2005) 35.

29 King S W, French M, Bielefeld J & Lanford W A, Fourier transform infrared spectroscopy investigation of chemical bonding in low-k a-SiC:H thin films, *J Non Cryst Solids*, 357 (2011) 2970.

30 Sylvestre S, Sebastian S, Edwin S, Amalanathan M, Ayyapan S, Jayavarthanan T, Oudayakumar K & Solomon S, Vibrational spectra (FT-IR and FT-Raman), molecular structure, natural bond orbital, and TD-DFT analysis of l-Asparagine monohydrate by density functional theory approach, *Spectrochim Acta Part A Mol Biomol Spectrosc*, 133 (2014) 190.

31 Panneerselvam A, Arumugam R, Ramasamy S, Valarmathi N & Geetha D, Removal of methyl orange and methylene blue from wastewater by magnetic nanocomposites loaded activated carbon synthesised from walnut shell, *Indian J Chem Technol* 31 (2024) 355.

32 Mekonnen B Y, Fentaw D A. & Zeleke M A, Synthesis and characterization of ZnO/activated carbon khat nanocomposite for removal of methylene blue dye, *Indian J Chem Technol*, 31 (2024) 462.

33 Elmerzouki, K., Bimaghra, I., Sahlaoui, A., Lghazi, Y & Himi M A, Adsorption of organic dye methylene blue on activated carbon prepared from wood, *Int J Eng Technol*, 7 (2018) 32.

34 Uma, Pandey A, Sharma Y C, Saleh B, Comparative studies of removal of hazardous dyes (MB and MG) by low cost activated carbon, *Indian J Chem Technol*, 28 (2021) 297.

35 Valliammai S, Subbareddy Y, Nagaraja K S & Jeyaraj B, Removal of Methylene Blue from aqueous solution by activated carbon of Vigna mungo L and Paspalum scrobiculatum: equilibrium, kinetics and thermodynamic studies, *Indian J Chem Technol*, 24 (2017) 134.

36 Thakare S S, Shinde S T, Pawar R S, Sonawane K G & Kale A, Adsorption of methylene blue using untreated biosorbent prepared from Geranium plant waste: Isothermal, kinetic and thermodynamic study, *Indian J Chem Technol*, 31 (2024) 571.

37 Yorgun S, Karakehya N & Yildiz D, Adsorption of methylene blue onto $ZnCl_2$-activated Paulownia wood carbon: kinetic and equilibrium studies, *Desalin Water Treat*, 58 (2017) 274.

38 Dolas H, Activated carbon synthesis and methylene blue adsorption from pepper stem using microwave assisted impregnation method: Isotherm and kinetics, *J King Saud Univ Sci*, Published online, (2023).

39 Villegas-Peralta Y, González-Tineo P A, Duarte-Ruiz C A, Sánchez-Duarte R G, Martínez-Macias M, del R Dévora-Isiordia G E, Álvarez-Sánchez J & Flores-Aquino E, Chemistry activation of sawdust activated carbon for dye removal: kinetics and isotherms, *Desalin Water Treat*, 321 (2025) 100947.

40 Boltz R, Ziemnicka-Lak K, Pratt K D, Balasubramanian R & Agrawal A, Activated carbon from nutshells for methylene blue adsorption: Production, characterization, and performance compared with commercial carbons, *ACS Sustain Resour Manag*, 6 (2024) 1895.

41 Firdaus M L, Krisnanto N, Alwi W, Muhammad R & Serunting M A, Adsorption of textile dye by activated carbon made from rice straw and oil palm midrib, *Aceh Int J Sci Technol*, 6 (2017) 1.

42 Sivakumar V, Karthikeyan A & Selvapathy P, Dye adsorption using low-cost carbon adsorbent from agro-waste-pearl millet cob husk, *Indian J Chem Technol*, 26 (2014) 35.

43 Kini M S, Saidutta M B & Murty V R, Studies on biosorption of methylene blue from aqueous solutions by powdered palm tree flower (Borassus flabellifer), *Int J Chem Eng*, 2014 (2014) 306519.

44 Bhattacharyya K, Adsorption characteristics of the dye, brilliant green, on neem leaf powder, *Dye Pigment*, 57 (2003) 211

45 Abewaa M, Mengistu A, Takele T, Fito J & Nkambule T, Adsorptive removal of malachite green dye from aqueous solution using Rumex abyssinicus derived activated carbon, *Sci Rep*, (2023) 14701.

46 Konicki W, Aleksandrzak M, Moszyński D & Mijowska E, Adsorption of anionic azo-dyes from aqueous solutions onto graphene oxide: Equilibrium, kinetic and thermodynamic studies, *J Colloid Interface Sci*, 2017 (496) 188.

47 Mouni L, Belkhiri L, Bollinger J C, Bouzaza A, Assadi A, Tirri A, Dahmoune F, Madani K & Remini H, Removal of Methylene Blue from aqueous solutions by adsorption on Kaolin: Kinetic and equilibrium studies, *Appl Clay Sci*, 153 (2018) 38.